ACS APPLIED MATERIALS & INTERFACES

Research Article

www.acsami.org

# Fabrication and Characterization of Heparin-Grafted Poly-L-lactic acid–Chitosan Core–Shell Nanofibers Scaffold for Vascular Gasket

Ting Wang,[†,‡] Xuyuan Ji,[†] Lin Jin,[†,§] Zhangqi Feng,[†,§] Jinghang Wu,[#] Jie Zheng,[∥] Hongyin Wang,[†] Zhe-Wu Xu,[⊥] Lingling Guo,[†] and Nongyue He*[,†]

[†]State Key Laboratory of Bioelectronics, School of Biological Science and Medical Engineering, Southeast University, Nanjing 210096, China

[‡]First Affiliated Hospital of Jinan University, Guangzhou 510630, China

[§]School of Engineering, Sun Yat-Sen University, Guangzhou 510006, China

[⊥]Department of Oral and Maxillofacial Surgery, Guanghua School of Stomatology, Sun Yat-Sen University, Guangzhou, China

[#]The Dow Chemical Company, Midland, Michigan 48674, United States

[∥]Department of Chemical and Biomolecular Engineering, The University of Akron, Akron, Ohio 44325, United States

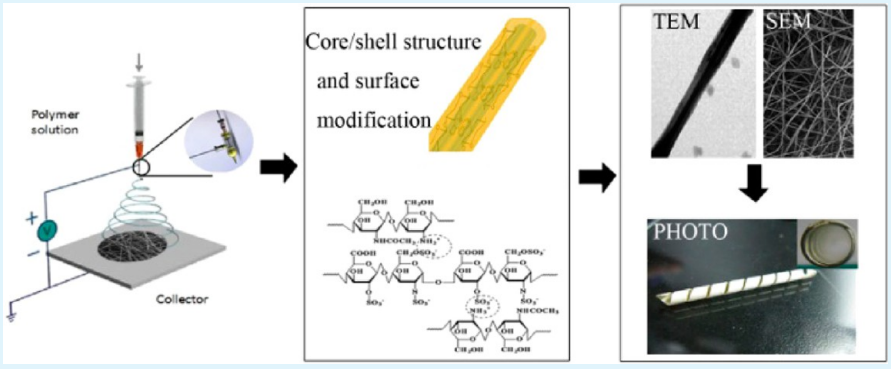


**ABSTRACT:** Electrospun nanofibers were widely studied to be applied as potential materials for tissue engineering. A new technology to make poly-L-lactic acid/chitosan core/shell nanofibers from heterologous solution by coaxial electrospinning technique was designed for vascular gasket. Chitosan surface was cross-linked by genipin and modified by heparin. Different ratios of PLA/CS in heterologous solution were studied to optimize the surface morphology of fibers. Clean core–shell structures formed with a PLA/CS ratio at 1:3. Superior biocompatibility and mechanical properties were obtained by optimizing the core–shell structure morphology and surface cross-linking of chitosan. UE7T-13 cells grew well on the core–shell structure fibers as indicated by methylthiazolyldiphenyl-tetrazolium bromide (MTT) results and scanning electron microscopy (SEM) images. Compared with the pure PLA fiber meshes and commercial vascular patch, PLA/CS core–shell fibers had better mechanical strength. The elastic modulus was as high as 117.18 MPa, even though the yield stress of the fibers was lower than that of the commercial vascular patch. Attachment of red blood cell on the fibers was evaluated by blood anticoagulation experiments and in vitro blood flow experiments. The activated partial thromboplastin time (APTT) and prothrombin time (PT) value from PLA/CS nanofibers were significantly longer than that of pure PLA fibers. SEM images indicated there were hardly any red blood cells attached to the fibers with chitosan coating and heparin modification. This type of fiber mesh could potentially be used as vascular gasket.

**KEYWORDS:** *electrospun nanofibers, core/shell structure, surface modification, chitosan, poly-L-lactic acid, biocompatibility*

## INTRODUCTION

A typical electrospinning device consists of a high voltage source supply, an electrically conducting spinneret (such as a syringe needle), and a grounded collector with a certain distance separated between the spinneret and collector. The jet formed by polymer solutions is ejected by a syringe needle with high electric potential supply and is then collected onto a grounded collection plate with low electric potential, during which time the fibers solidify and form onto the plate because of solvent evaporation. When the applied voltage is balanced with appropriate surface tension and viscosity, the fibers deposit onto the grounded target and form a nanofibrous mat.[1,2] Biodegradable polymers, such as poly(D, L-lactic) acid, polyglycolic acid, and their copolymers have drawn a lot of attention in research worldwide because of their better biocompatibility and degradability properties.[3−6] These materi-

Received: January 28, 2013
Accepted: April 15, 2013
Published: April 15, 2013

 © 2013 American Chemical Society 

als prepared by electrospinning[7−9] have also been chosen to serve as scaffolds for bone tissue and vessel, and patches for wounds.[10,11] Derived mainly from plants, PLA is one of the most widely used polymers and can be metabolized in human body. It has been already approved by the Food and Drug Administration (FDA) to be used in surgical sutures, microcapsules, microspheres and implant agent materials.[12,13] However, PLA is brittle under tensile load, which is an undesirable characteristic in applications such as biomedical filters or tissue scaffolds. Thus fabricating PLA fibers with enhanced mechanical properties and biocompability would lift the limitation of applying PLA into these applications.

Chitosan is the second-most abundant natural polysaccharide after cellulose. It is normally embedded in the protein matrix of crustacean shells and squid pens.[14] Chitosan has characteristics similar to glycosaminoglycans, such as biocompatibility, biodegradability, antimicrobial activity, wound healing properties, antitumor effects, and so on.[15] Electrospun Chitosan fibers have been used in many biomedical fields such as skin, bone or certilage,[16,17] because of their excellent biological properties. Techniques of fabricating chitosan by electrospinning have been reported by Feng et al. and Yamamoto et al.[18,19] Some other chitosan-based nanoparticles or nanofibers were also reported to be applied as biomaterials.[20,21]

To impart different properties to the resultant nanofibres, coaxial electrospinning technologies were used. Coaxial electrospinning technologies were usually applied to enhance or endow biomaterials with functionalized property for different applications, such as, nylon/$ZnO_2$ core−shell fibers,[22] or polypeptide core−shell fibers.[23] In this study, to improve the mechanical property and biocompatibility of electrospun nanofiber mats, coaxial electrospinning technology was employed to fabricate poly-L-lactic acid (PLA)/chitosan (CS) core−shell nanofiber mats, in which CS served as the shell due to its excellent biocompatibility comparing to PLA. The testing of cyto-compability and antithrombogenicity was carried out to study the improvement of CS on biocompability and hemolytic properties of the nanofiber mats.

## MATERIALS AND METHODS

**Materials.** Commercial samples, Chitosan-200 ($M_W$ = 200 kDa, deacetylation of the chitosan is 85%) were purchased from Haidebei Marine Bio Ltd. (Jinan, China). PEO (Biogrand, $M_W$ = 1000 kDa) was obtained from Guoren Chemical Ind. (Beijing, China). PLA ($M_w$ = 5 × $10^6$ Da) was purchased from Daigang Biological Technology Co. (Shandong, China). Formic acid (HCOOH, ∼99% purity) and ethanol absolute were purchased from Jiuyi Chemical Ind. (Shanghai, China). All the reagents were analytical reagent grade. Vascu-Guard vascular patch as commercialized control provided from Nanjing Drum Tower Hospital.

**Methods.** A special syringe needle was designed for making the electrospun nanofibrous structure. A double layer syringe needle was designed for solutions with different polarity as shown in Figure 1B. PLA solutions were made by dissolving PLA into dichloromethane at certain mass ratios. The chitosan solution (CS) was prepared by dissolving different quantities of chitosan powder and poly(ethylene oxide) (PEO) into formic acid solution (2%) at 70/30 wt ratio by magnetic string, this mixture solution was called CS solution in the following discussion. PLA and CS solution were then pumped into the syringe separately with 10 kV of electric potential applied to the metallic needle (Figure 1B) using a DC power supply. The electrostatically charged fibers with core−shell structure (Figure 1C) were ejected toward a plate collector, which was covered with aluminum foil. The PLA/CS mat was then collected onto the collector (Figure 1A). The feeding speeds for both of spinning solutions were 5 mL/h. The distance between the needle and the collector was around 18 cm with a relative humidity at around 40% under ambient conditions at 25 °C. The spinning time of spinning solutions was controlled to produce mats in appropriate thickness ranges. The collected electrospun mats were held at room temperature for at least 24 h to ensure complete drying of the samples. PLA/CS core−shell electrospun nanofibrous membranes were cross-linked by spraying genipin solution onto the mats at room temperature for 3 h. Genipin solution was prepared by dissolving genipin in a mixture of acetone (A) and water (W), A to W is 3 to 7. After that, fibers were immersed in heparin solutions for further cross-linking. Excess amount of deionized water was used to wash away untreated chemicals after the cross-linking reaction. The cross-linked membranes were dried at 45 °C in a vacuum chamber for 24 h and ready for further cell culture and in vitro adhesion study.

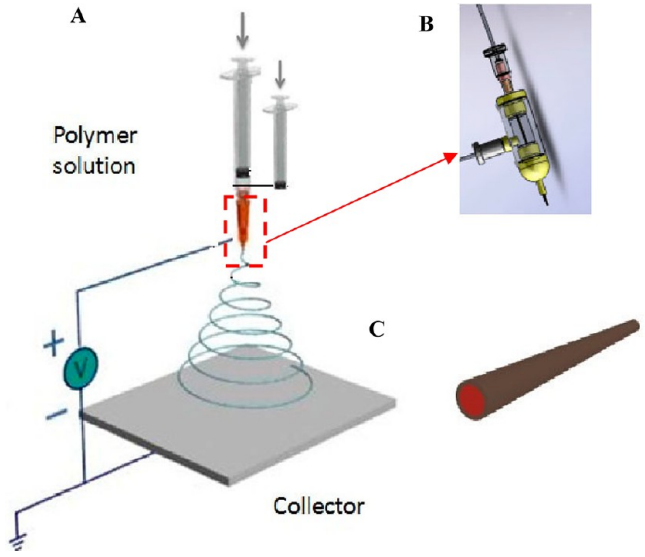


**Figure 1.** (A) Illustration of polymer electrospun, (B) illustration of house made syringe needle, (C) illustration of fibers with core−shell structure.

**Morphology of Chitosan Nanofibers.** The morphology of chitosan nanofibers was examined by a scanning electron microscope (SEM; Hitachi SN-3000N, Japan) at an acceleration voltage of 20 kV. Statistical analysis on average diameter and diameter distribution of nanofibers were obtained from SEM images. The core−shell structure of the nanofibers was characterized by transmission electron microscopy (TEM, JEM3010 JEOL) with an acceleration voltage of 30 to 300 kV.

**Surface Tension and Viscosity Measurements.** The viscosity of CS solutions in aqueous formic acid was measured in a shear rate range of 5−500 $s^{-1}$ using a Haake Viscometer (VT550) equipped with double concentric cylinder-type SP2P sensors. The surface tension was measured by the maximum bubble pressure method.[1]

**FTIR.** The infrared spectra of PLA and PLA/CS core−shell fiber were collected with an attenuated reflectance Fourier Transform (Excalibur FTS- 3000) spectrometer. Transmission mode with PLA and PLA/CS mesh was used for bulk chitosan and chitosan nanofibers samples. All spectra were scanned across a wavenumber range from 4000 to 500 $cm^{-1}$ with accumulation of 64 scans and a resolution of 4 $cm^{-1}$.

**Blood Anticoagulation.** Fresh blood (30 mL) was collected from healthy rabbits in accordance with institutional policies. The whole blood with odium citrate (0.109 mol/L) was sedimentated by centrifugation at 800 g for 20 min and platelet-rich plasma (PRP) above the buffy coat was then gently removed; 2500 g of the PRP was then centrifugated for 15 min to get the platelet-poor plasma (PPP). PLA/CS films in saline solution (0.9% w/v NaCl) were cut into 10 × 10 mm pieces (0.005 g) and placed in a tissue culture well (12-well plates, Becton Dickinson, Franklin, NJ) with blood pressure kept at

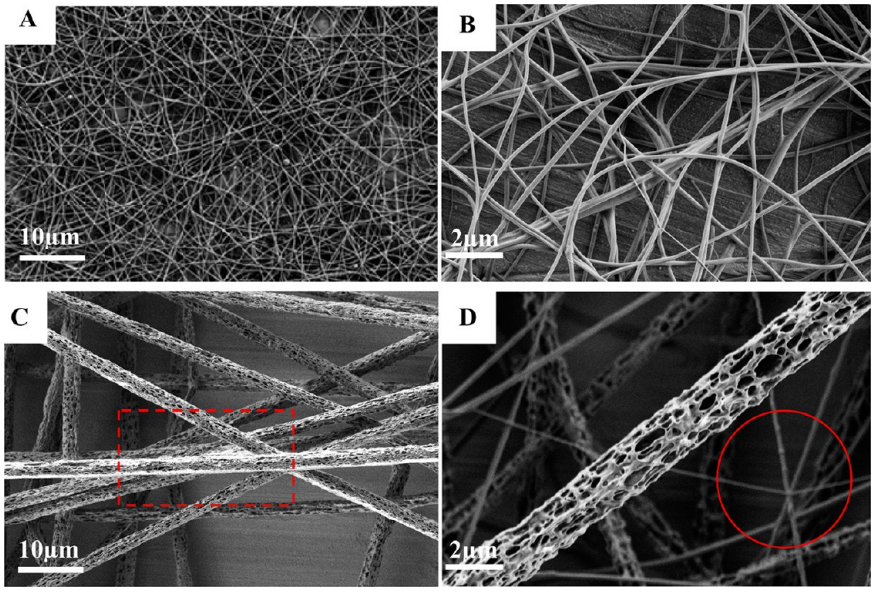


**Figure 2.** Surface morphologies for electrospinn:ing fibers (A) SEM image for PLA/CS (1:3) core/shell fibers. (B) SEM image for PLA/CS (1:3) core/shell fibers produced with higher magnification. (C) SEM image for fibers with PLA/CS (1:1); as shown in the red square, the fibers agglomerate obviously; (D) SEM image for PLA/CS (1:1), the fibers with higher magnification; as shown in the red circle, the diameters of the fibers were not uniform.

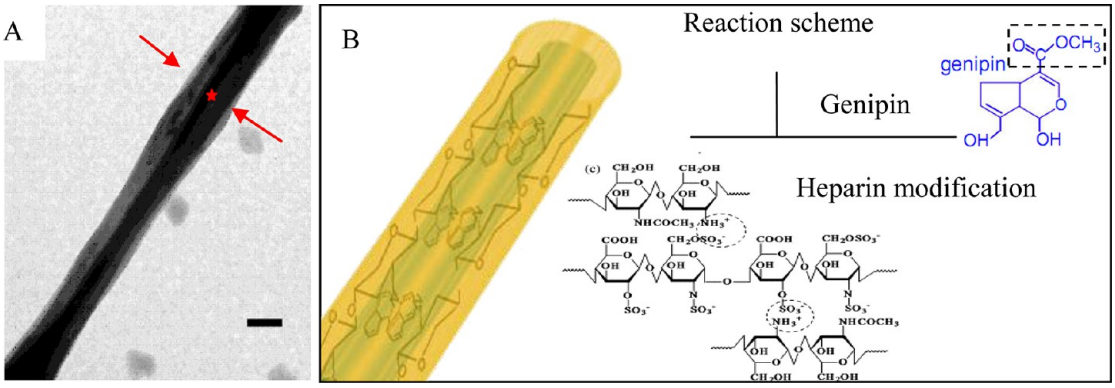


**Figure 3.** (A) TEM image of CS-PLA coaxial fibers. Core and shell part are indicated by asterisk and arrows, respectively (scale bar is 100 nm). (B) Surface reaction scheme for the core structure.

0.08 mmHg and incubated at 37 °C for 1 h. The activated partial thromboplastin time (APTT) and prothrombin time (PT) were evaluated in vitro by a blood coagulation analyzer (RT-2204c, Rayto Life and Analytical Sciences Co., Ltd., China). The saline solution was used as blank control. Every sample was tested three times to get an average value.

**In Vitro Blood Flow Experiments.** Whole blood experiment was carried out under flow conditions using a modified Chandler-Loop. The system consists of a thermostatted water bath connecting to a rotating unit by polyvinyl chloride loops. In this experiment, 12 samples were prepared in the chamber with 50 mL fresh whole blood from healthy rabbits filled in. The loops were cycled at 30 rpm at 37 °C for 1 h, achieving a flow rate of 65 mL/min. The blood was then replaced and the physiological saline was used to rinse the loop for 15 min under the same conditions afterward. The fiber meshes with red blood cells were fixed using 2.5% glutaraldehyde solution for 12 h. Ethanol solutions of 25, 50, 75, 90, and 100% were used stepwise to dehydrate the red cells on the mesh with each step for 15 min. Finally, the samples were coated with thin layers of gold via sputtering and examined by scanning electron microscopy (SEM; Hitachi SN-3000N, Japan).

**Cell Culture.** Human bone marrow-derived UE7T-13 cells were cultured in dulbecco's minimum essential medium (DMEM) supplemented with 10% newborn calf serum (NBCS) with 1% Penicillin-Streptomycin solution, and incubated at 37 °C/5% $CO_2$. PLA as a control group and PLA/CS core−shell structure mats as experiment group were ultraviolet sterilized and placed in a 96-well tissue culture plate. UE7T-13 cells were suspended in DMEM at $1 \times 10^5$ cells $mL^{-1}$ and 20 $\mu$L cells suspension were planted on the electrospun mats. The medium was changed every two days during incubation at 37 °C/5% $CO_2$. Cell proliferation on each sample was tested after 1, 4, and 7 days by MTT assay.

**Mechanical Properties.** Mechanical properties of the samples were evaluated by an electronic universal testing machine (Instron 5943, USA). The sample size was 6 cm × 1 cm with 40 mm of gauge length and 5 mm/min of clamp speed.

**Statistical Analysis.** Data were expressed as the mean ± standard deviation. Statistical analyses were performed using the *t*-test. All data were analyzed with SPSS software (version 11.0).

## RESULTS AND DISCUSSION

### Surface Tension and Viscosity of CS and PLA Solution.

*Surface Character.* The composition of the electrospinning solution controls the surface tension of liquid. Surface tensions together with the evaporation rate of the solution are important


dx.doi.org/10.1021/am400369c | ACS Appl. Mater. Interfaces 2013, 5, 3757−3763

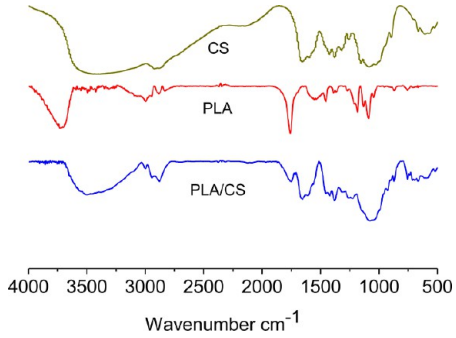


**Figure 4.** ATR-FTIR for pure CS, pure PLA, and PLA/CS nanofibers.

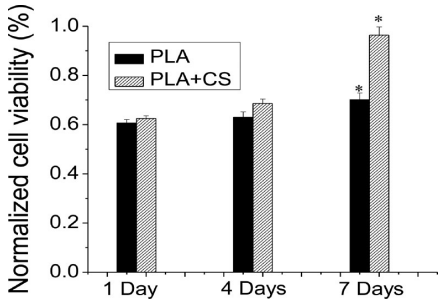


**Figure 6.** MTT for cell culture, (*): $p < 0.05$.

parameters affecting the formation of droplets, beads and fibers. Based on previous work,[1] we optimized the results and selected two types of CS soluton (3 and 1 wt %) with surface tension and viscosity at 45 dyn/cm, 307 mPa s and 30 dyn/cm, 270 mPa s, respectively, PLA solution (1 wt %) at 55 dyn/cm, 504 mPa s respectively. We used different ratios of CS and PLA (wt) from different channels of the double-layer syringe needle for PLA/CS core−shell structure to optimize the surface structure and mechanical properties of the vascular gasket.

The relative quantity of CS and PLA is a strong factor influencing the surface structure of the fibers. Different fiber surface morphology was obtained when different ratios of PLA and CS solutions in two different syringe channels were used at 1:1 and 1: 3 (wt), respectively, under the same fabrication. As shown in Figure 2, when the amount of CS was three times more than the PLA, fibers exhibited smooth surface with homogeneous morphology (Figure 2A, B) compared to the rough and porous fibers obtained from a solution with a 1:1 PLA/CS ratio (Figure 2C, D). Fibers produced with a 1:3 PLA/CS ratio in images A and B in Figure 2 have an average diameter at about 200 nm, compared to 2 $\mu$m for that of the fibers produced from the solution with a 1:1 PLA/CS ratio as shown in Figure 2 C. As shown in Figure 2D, the fibers produced from a solution with a CS/PLA of 1:1 exhibited poor characteristics. The fibers were not uniform with porous surface structure and probably resulted from an inhomogeneous morphology (Figure 2C, D).

TEM image in Figure 3A demonstrated smooth surface and clear core−shell structure of PLA/CS core−shell fiber and the shell was composed of CS with the core made by PLA. The CS on the outside of the fiber is translucent and PLA core showed higher contrast. Mechanisms of surface cross-link and charge effect for heparin modification were illustrated in Figure 3B.

The coaxial pinhead facilitated the core−shell structure of the nanofibers. Surface cross-linking improves the mechanical strengths of the fibers. The core−shell structure of the fibers formed from the double layer structure of needles and is caused by the phase separation between CS and PLA, since CS and PLA were dissolved in different homogeneous solutions. Another explanation for possible accumulation of CS phases on the surface of the fiber might be due to easy movement of the positively charged CS groups under the electrical field during electrospinning.[3] Ratio of CS and PLA can be used to tailor the surface morphology of nanofibers. Mechanical integrity of the fibers can be controlled by their surface morphology. To optimize this surface morphology, we used the ratio of PLA/CS 1:3 in the following study.

*FTIR Experiment.* Fourier transforms infrared spectroscopy (FTIR) data characterizes important information about the intermolecular and intramolecular interactions in polymers. Figure 4 showed the FTIR spectra of pure PLA, pure chitosan electrospun fibers comparing to PLA/CS core−shell fibers with chemical modification. For PLA fiber the band at 1400 $cm^{-1}$ is attributed to the −CO single bond from the −COO group of PLA. For chitosan fiber the characteristic band at 1594 $cm^{-1}$ was contributed by I and II amides from CS. In the PLA/CS core/shell fibers with chemical modification, we can find the band at 1400 $cm^{-1}$ from −COO group of PLA, with the peaks at 1594 $cm^{-1}$ contributed by I and II amides from CS, and the strong peaks in 1060 originated from $-SO_3$ in heparin (HS).

*Mat and Scaffold.* The flat fiber mats was twisted round the glass rod to form a scaffold. The scaffolds were then prepared by cross-linking the surface of the fiber mat. The scaffold were taken off the glass with a wire spring shape (Figure 5A) after the mat surface was cross-linked. The morphological details of the nanofibers in the mat were shown in Figure 5B. As seen from the SEM image, the fibers were separate from each other and exhibited homogeneous surface morphology.

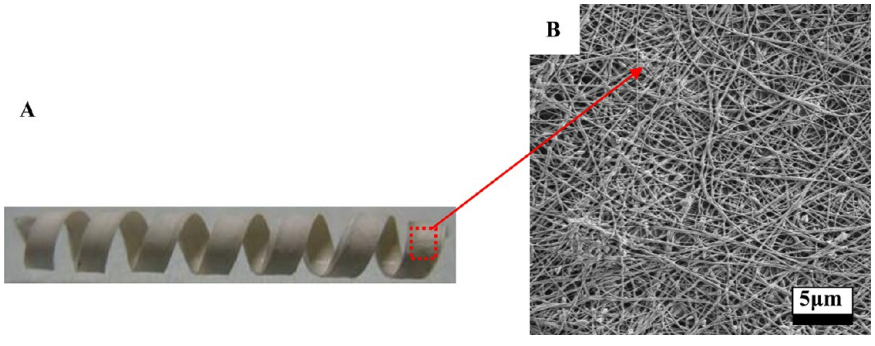


**Figure 5.** (A) Scaffold made from PLA/CS nanofiber mat, (B) SEM image for PLA/CS core/shell nanofibers.

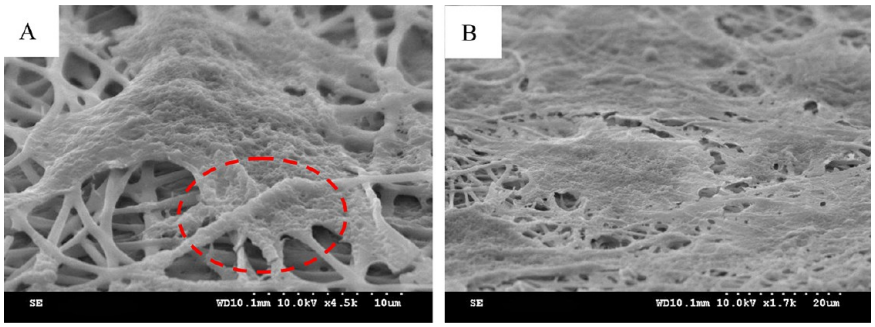


**Figure 7.** SEM images of cells on the PLA/CS scaffold: (A) cells pseudopod labeled with red circle after being cultured for 1 day, (B) large quantity of cells found on the scaffold after being cultured for 7days.

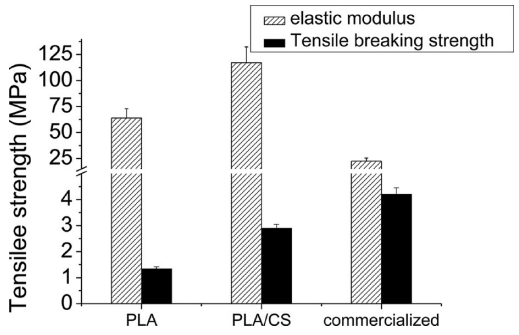


**Figure 8.** Elastic modulus and tensile breaking strength (yield stresses) of the three different types of scaffolds.

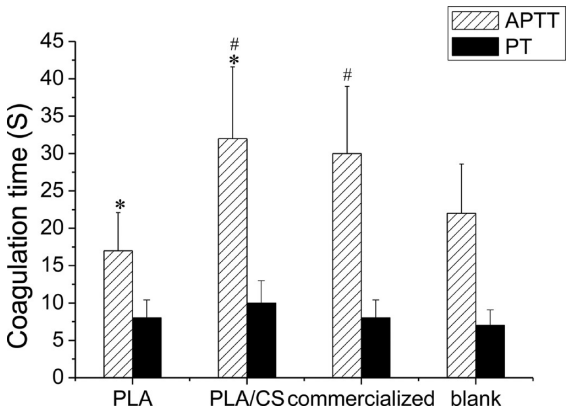


**Figure 9.** APTT, PT value for different type of mesh, (*): $p < 0.05$, ($^{\#}$): $p > 0.05$.

*Cell Culture.* The attachment, activity, and morphology of human bone marrow-derived UE7T-13 cells were used to evaluate the compatibility of nanofibers on the cellular level as an indication of the biocompatibility of the electrospun CS/PLA nanofibers. Cell viability was assessed using a MTT assay. The Medical Devices Quality Management Systems Requirements for Regulatory Purposes of China 2010.6 were used as criteria for evaluation of the cellular compatibility of nanocapsules. The results are discussed in the following sections.

The relative growth rate (RGR) of cells was over 90% on PLA/CS nanofibers compared to 70% of that on PLA fiber RGR of cells on the seventh day with the statistic analyze $p < 0.05$ can be found (Figure 6). From the Medical Devices Quality Management Systems Requirements for Regulatory Purposes of China 2010.6, the experimental materials were considered to be nontoxic, if the RGR of cells is greater than 80% in 7 days culture. The morphology of cellbeing monitored should be observed.

From the MTT results, we found that the cells on PLA did not grow well. From the fourth day to the seventh day, the quantity of the cells viability on nanofibers increased very slowly (from 63.7% to 70.3%) which might have been influenced by PLA degradation.[24] PLA is a manmade, biodegradable polymer. The degradation products of PLA are acidic, which will influence the pH value of cell-culture medium. Uncomfortable environment in cell-culture medium can be one of the reasons to slow down the cell generation speed. At the same time, the cells grown on PLA/CS nanofibers looked better. Quantity of the cells increased from 68 to 92.4% in three days. These results indicated that PLA/CS nanofibers with surface cross-linking and modification exhibited good biocompatibility.

To evaluate the biocompatibility of the electrospun PLA/CS nanofibers, we evaluated adhesion, activity, and morphology of the cells cultured on the mesh. The detailed morphology of cells cultured on PLA/CS fibers for 1 day and 7 days is compared in SEM images A and B in Figure 7, respectively. As shown in Figure 7A, the pseudopod morphology can be found spreading onto the fibers, which indicates that pseudopod projection and extent of cell spreading were increasing.

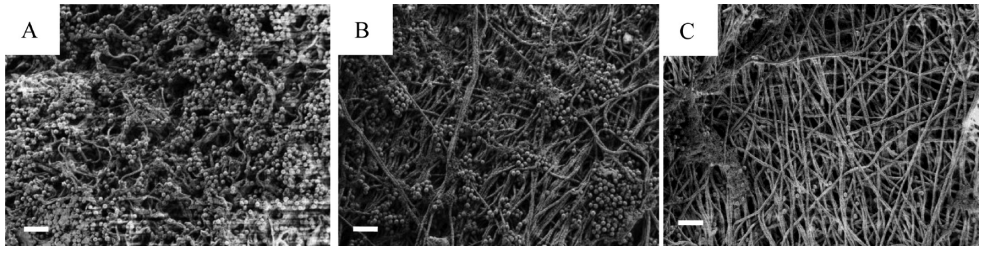


**Figure 10.** SEM image for red blood cell adhesion on the surface of the mat (scale bar is 50 $\mu$m): (A) PLA nanofiber mesh, (B) commercialized vascular patch, (C) PLA/CS core/shell nanofiber.


dx.doi.org/10.1021/am400369c | ACS Appl. Mater. Interfaces 2013, 5, 3757−3763

After being cultured for 7 days (Figure 7 B), the image showed widespread cells on surface of the fibers, large quantity of cells connected to neighboring cells. A two-dimensional monolayer of extensive cell−cell contacts formed. Close adherence of cells to the chitosan fiber and protein fibers attachments of the cells can be seen from the image. Combined with the results from MTT, we conclude that the modified PLA/CS nanofibers mesh has good biocompatibility with UE7T-13 cells. Thus this type of mesh can be potentially used as a culture substrate for stem cells in tissue.

*Mechanical Property*. PLA/CS nanofibers with surface cross-linking and modification influenced the elastic modulus of the fibers. The modulus of the fibers was examined by an instron electronic universal testing machine. The results (Figure 8) showed that the yield stress of the PLA/CS nanofibers was higher than that of the pure PLA fibers. Moreover, with surface cross-linking, elastic modulus of the fibers increased dramatically to around 117.18 MPa. These results showed that the surface cross-linking and modification enhanced the mechanical strength of the fibers. Elastic modulus of the fibers increased after the PLA/CS core−shell nanofibers were surface cross-linked by genipin, whereas the yield stress of PLA/CS nanofibers decreased after cross-linking. Chitosan agglomerated within the fibril network and was subsequently cross-linked by spraying genipin on the surface of the fibers. The commercialized vascular patch showed a relatively low elastic modulus but high yield stress.

**Blood Clotting Time of Fibers.** The activated partial thromboplastin time (APTT) and prothrombin time (PT) value in Figure 9 showed the coagulation time of the blood was prolonged by chitosan surface, which was similar to that of commercial vascular patch (APTT and PT for PLA/CS vascular gasket are 32 s, 9.2 s, those for the commercialized vascular patch are 30 s, 8.0 s). Heparin modified on the chitosan surface is one of the reasons for prolonged blood coagulation time.

From the in vitro blood flow experiments histogram, (Figure 10), we found that large quantities of red blood cells adhered onto pure PLA fibers after 4 h, blood flowing at 37 °C (Figure 10 A). When commercial vascular patch was used, red blood cells can still be found on the fibers but in smaller quantity comparing to that on the pure PLA fibers. With the heparin modification on the surface of PLA/CS mat, the mesh exhibited good blood compability and low blood coagulation. Under SEM imaging, few cells can be found in the crevice of the fibers. Thus, PLA/CS core−shell nanofibers are suitable for being applied as anticoagulant biomaterials as well. These benefits might be brought by heparin, which was covalently bonded onto the surface of the fibers during surface cross-linking process.

## CONCLUSION

Coaxial technology allows PLA in dichloromethane solution and chitosan in acid aqueous solution to fabricate core−shell structure nanofibers. Mechanical properties of the electrospun nanofiber mats were enhanced by the PLA in core of the fiber and surface cross-linking on the CS shell by genipin. Biocompatibilities of the fiber were improved from CS shell with heparin modification on the surface. As discussed above, core−shell structure enhanced the elastic modulus of the fiber as high as 117.18MP, which was similar to commercial vascular patch. With the heparin modification on CS shell, fibers exhibited great anticoagulant activity. APTT and PT value reached 32 s and 9.2 s, which was close to that of commercial vascular patch ($p > 0.05$). These results can be confirmed by SEM images where red blood cell adhered well onto three different types of fibers. In conclusion, PLA/CS core−shell scaffold can be a good candidate for being applied as biomaterials in intravascular stent.

## AUTHOR INFORMATION

### Corresponding Author

*E-mail: nyhe@seu.edu.cn. Tel.: +86 25 83790885. Fax: +86 25 83790885.

### Notes

The authors declare no competing financial interest.

## ACKNOWLEDGMENTS

This work was supported by NSFC (11204033, 51103181, 61271056), the Research Fund for the Doctoral Program of Higher Education of China (20120092120042), the Fundamental Research Funds for the Central Universities, the project of Science & Technology New Star of Zhu Jiang in Guangzhou city, and Open Fund of The First Affiliated Hospital, Jinan University Guangzhou, and Open Research Fund of State Key Laboratory of Bioelectronics, Southeast University.

## REFERENCES

(1) Feng, Z. Q.; Leach, M. K.; Chu, X. H.; Wang, Y. C.; Tian, T.; Shi, X. L.; Ding, Y. T.; Gu, Z. Z. *J. Biomed. Nanotechnol.* **2010**, *6*, 658−66.
(2) Feng, Z. Q.; Chu, X. H.; Huang, N. P.; Wang, T.; Wang, Y. C.; Shi, X. L.; Ding, Y. T.; Gu, Z. Z. *Biomaterials* **2009**, *30*, 2753−63.
(3) Li, Y. J.; Chen, F.; Nie, J.; Yang, D. Z. *Carbohydr. Polym.* **2012**, *90*, 1445−51.
(4) Jin, L.; Wang, T.; Feng, Z. Q.; Zhu, M. L.; Leach, M. K.; Naim, Y. I.; Jiang, Q. *J. Mater. Chem.* **2012**, *22*, 18321−26.
(5) Wang, T.; Feng, Z. Q.; Leach, M. K.; Wu, J. H.; Jiang, Q. *J. Mater. Chem. B.* **2013**, *1*, 339−46.
(6) Chen, Q.; Pugno, Nicola. M. *Compos., Part B* **2011**, *42*, 2030−37.
(7) Jin, L.; Feng, Z. Q.; Zhu, M. L.; Wang, T.; Leach, M. K.; Jiang, Q. *J. Biomed. Nanotechnol.* **2012**, *8*, 779−85.
(8) Jin, L.; Wang, T.; Zhu, M. L.; Leach, M. K.; Naim, Y. I.; Corey, J. M.; Feng, Z. Q.; Jiang, Q. *J. Biomed. Nanotechnol.* **2012**, *8*, 1−9.
(9) Feng, Z. Q.; Lu, H. J.; Leach, M. K.; Huang, N. P.; Wang, Y. C.; Liu, C. J.; Gu, Z. Z. *Biomed. Mater.* **2010**, *5*, 065011−19.
(10) Zhang, Y. Z.; Su, B.; Venugopal, J.; Ramakrishna, S.; Lim, C. T. *Int. J. Nanomed.* **2007**, *6*, 623−38.
(11) Srikar, R.; Yarin, A. L.; Megaridis, C. M .; Bazilevsky, A. V.; Kelley, E. *Langmuir* **2008**, *24*, 965−74.
(12) Lee, S.; Leach, M. K.; Redmond, S. A.; Chong, S. Y. C.; Mellon, S. H.; Tuck, S. J.; Feng, Z. Q.; Corey, J. M.; Chan, J. R. *Nat. Methods* **2012**, *9*, 917−22.
(13) Majeti, N. V.; Kumar, R. *React. Funct. Polym.* **2000**, *46*, 1−27.
(14) Wang, T.; Hu, Y.; Leach, M. K.; Zhang, L.; Yang, W. J.; Jiang, L.; Feng, Z. Q.; He, N. Y. *Int. J. Pharm.* **2012**, *422*, 462−71.
(15) Bispo, V. M.; Mansur, A. A. P.; Barbosa-Stancioli, E. F.; Mansur, H. S. *J. Biomed. Nanotechnol.* **2010**, *6*, 166−75.
(16) Duan, B.; Dong, C.; Yuan, X.; Yao, K. *J. Biomater. Sci.−Polym. Ed.* **2004**, *15*, 797−811.
(17) Alves, N. M.; Mano, J. F. *Int. J. Biol. Macromol.* **2008**, *43*, 401−14.
(18) Charernsriwilaiwat, N.; Opanasopit, P.; Rojanarata, T.; Ngawhirunpat, T. *Int. J. Pharm.* **2012**, *427*, 379−84.
(19) Ohkawa, K.; Cha, D.; Kim, H.; Nishida, A.; Yamamoto, H. *Macromol. Rapid Commun.* **2004**, *25*, 1600−05.
(20) Wang, T.; He, N. Y. *Nanoscale* **2010**, *2*, 230−9.
(21) Fu, J.; Wang, D. X.; Wang, T.; Yang, W. J.; Deng, Y.; Wang, H.; Jin, S. G.; He, N. Y. *J. Biomed. Nanotechnol.* **2010**, *6*, 725−8.
(22) Fatma, K.; Cagla, O.; Inci, D.; Necmi, B.; Tamer, U. *ACS Appl. Mater. Interfaces* **2012**, *4*, 6185−94.

(23) Khadka, D. B.; Cross, M. C.; Haynie, D. T. *ACS Appl. Mater. Interfaces* **2011**, *3*, 2994−3001.
(24) Li, J.; Kong, M.; Cheng, X. J.; Li, J. J.; Liu, W. F.; Chen, X. G. *Int. J. Biol. Macromol.* **2011**, *49*, 1016−21.